Journal of Materials Chemistry C

PAPER

View Article Online
View Journal | View Issue

Cite this: J. Mater. Chem. C, 2014, 2, 1730

Low-voltage blue-phase liquid crystals with polyaniline-functionalized graphene nanosheets

Shuibin Ni,[a] Hongjing Li,[a] Shuang Li,[b] Jiliang Zhu,[a] Jian Tan,[a] Xiaoyang Sun,[a] Chao Ping Chen,[a] Gufeng He,[a] Dongqing Wu,[b] Kuan-Cheng Lee,[c] Chang-Cheng Lo,[c] Alan Lien,[d] Jiangang Lu*[a] and Yikai Su[a]

Received 30th October 2013
Accepted 19th December 2013

DOI: 10.1039/c3tc32138j

www.rsc.org/MaterialsC

A small amount of polyaniline functionalized graphene (G–PANI, 0.03–2.00%) nanosheets was doped into conventional polymer-stabilized blue phase liquid crystals (PS-BPLCs), and the electro-optical property effects were studied. The driving capability of BPLCs can be much improved in that the Kerr constant of BPLCs doped with 0.05 wt% G–PANI is increased by ~55% compared with that of BPLCs without G–PANI. Meanwhile, this composite exhibits no degradation of electro-optical properties, such as response time, hysteresis and residual birefringence.

Introduction

Blue phase liquid crystals (BPLCs) appear as a regular array of double twist cylinders (DTCs) separated by a network of disclination lines in a narrow temperature range, 1–2 K, between the isotropic and chiral nematic (N*) phases.[1,2] The BPLC has interesting features including sub-millisecond response time, alignment free, optical isotropic status without an electric field, and 3-D helical structure with a periodicity on the order of the visible wavelength. Since the temperature range was broadened to more than 60 K by stabilizing the disclination lines with polymer networks,[3] BPLCs have attracted people's interest for potential applications in field sequential displays,[4,5] phase modulator devices,[6–9] and three-dimensional (3-D) tunable photonic crystals.[10,11] However, some critical issues, such as high driving voltage, hysteresis, and residual birefringence must be solved before they can be widely applied.[12,13] The hysteresis effect can be mitigated by doping ferroelectric ($BaTiO_3$) or ZnS nanoparticles,[14,15] but the driving voltage is still the main problem to be overcome before the wide applications of BPLCs. Generally, there are two methods to lower the driving voltage. One is to improve the materials which include large Kerr constant BPLC materials[16,17] and polymer systems with reactive diluents.[18] Another is to increase the effective electric field by device structure optimization, such as protrusion electrodes,[19] wall-shaped electrodes,[20] corrugated electrodes[21] and vertical field switching (VFS) electrodes.[22] In spite of their remarkable achievements in reducing the driving voltage, other problems, such as complicated fabrication processes and noticeable hysteresis need to be resolved eventually.

In recent years, graphene, a monolayer of carbon atoms arranged in a honeycomb network, has become an appealing carbon matrix owing to its excellent mechanical flexibility, large specific surface area,[23] and high thermal and chemical stability.[24–26] However, large scale production of high quality graphene still remains challenging using current technologies, including mechanical exfoliation, epitaxial growth on silicon carbide or metal surfaces, reduction of graphene oxide,[27] and liquid phase exfoliation.[28,29] Meanwhile, among those conducting materials, polyaniline is considered as a promising conductive material because of its low cost, easy synthesis and relatively high conductivity.[30] However, the polyaniline is prone to aggregation. Therefore, it is highly desirable to develop functionalized graphene nanosheets with unique structures that can tackle the aggregation of polyaniline while retaining the overall high conductivity and good dispersity.

In this work, the effect of polyaniline functionalized graphene (G–PANI) nanosheet doping on the electro-optical performance of polymer-stabilized blue phase liquid crystals (PS-BPLCs) is studied. The results show that with the G–PANI dopant of about 0.05% by weight, the Kerr constant of PS-BPLCs is increased by about 55%, and the response time, hysteresis, and residual birefringence have no degradation compared with those of PS-BPLCs without G–PANI.

[a]National Engineering Lab for TFT-LCD Materials and Technologies, Department of Electronic Engineering, Shanghai Jiao Tong University, Dongchuan Road 800, Shanghai, 200240, China. E-mail: lujg@sjtu.edu.cn
[b]School of Chemistry and Chemical Engineering, Shanghai Jiao Tong University, Dongchuan Road 800, Shanghai, 200240, China
[c]China Star Optoelectronics Technology Co. Ltd., Shenzhen, China
[d]TCL Corporation Research, China

Experimental

Mechanism

After polymerization, the driving capability of the PS-BPLCs will degrade obviously.[31] However, the polymer network is needed to solve the thermal stability problem of BPLCs. If the

conductivity of the polymer network can be increased, the effective electric field can be much improved to decrease the driving voltage of the PS-BPLC device. G–PANI nanosheets have unique structures that can tackle the aggregation of polyaniline while retaining relatively high conductivity and good dispersity. When the G–PANI nanosheets are doped into the BPLC materials, they can be wrapped by the polymer network around the disclination lines of blue phase liquid crystals. Therefore, the conductivity of the polymer system and the effective electric field of the PS-BPLC device will increase.

Material synthesis

Graphene oxide (GO) was synthesized from natural graphite flakes by a modified Hummers method.[32] The obtained GO was dispersed in the distilled water followed by hydrothermal treatment to get the graphene.

G–PANI: polyaniline functionalized graphene oxide nanosheets were prepared by *in situ* polymerization of aniline on GO, using sodium dodecyl sulfate (SDS) as the surfactant to assist the dispersibility of aniline in water: firstly, 300 μL aniline was dispersed in 50 mL distilled (DI) water with 10 mg SDS; then the mixture was mixed together with 60 mL of GO (0.50 mg mL^{-1}), followed by ultrasonication for 15 minutes to form a homogeneous suspension. Subsequently, 0.7 g ammonium persulfate (APS) dispersed in 50 mL 1 M HCl was added slowly, and the mixture was vigorously stirred overnight at 273–278 K. Then, the resulting green suspension was centrifuged and washed with DI water three times. The obtained GO–PANI was dispersed in 80 mL DI water followed by hydrothermal treatment at 453 K for 12 hours. Finally, the G–PANI nanosheets were obtained.

Material characterization

The morphology of G–PANI nanosheets was investigated by field emission scanning electron microscopy (FE-SEM). The TEM image reveals that the PANI layer on the surface of graphene is uniformly distributed and also the 2D sheets are freestanding. As the freestanding nanosheets can be easily dispersed into the mixtures, they are ideal materials for the modification of blue phase liquid crystals. Furthermore, the G–PANI composite is measured using a Fourier transform infrared spectrometer (FT-IR) as shown in Fig. 1(c), the peaks of –C═N, –C–N, and –N–H indicating the presence of PANI.

Samples preparation and measurements

The BPLC materials used in this experiment were composed of 88.75% of positive nematic LC (BPH001, HCCH), 3.17% of chiral dopant (R5011, HCCH), 3.39% of ultraviolet (UV)-curable monomer (12A, HCCH), 4.44% of cross-linker (C3M, HCCH), and 0.25% of photo-initiator (IRG184, HCCH) by weight. Then, different concentrations (0.03–2.00%) of G–PANI were doped into the above mixtures. After mixing, the mixtures were filled into in-plane switching (IPS) cells at an isotropic phase in a temperature controller (HCS302, Instec Co.). The cell gap of IPS cell is 7.5 μm. The indium tin oxide electrode width is 7.5 μm, and the electrode gap is 12.5 μm.

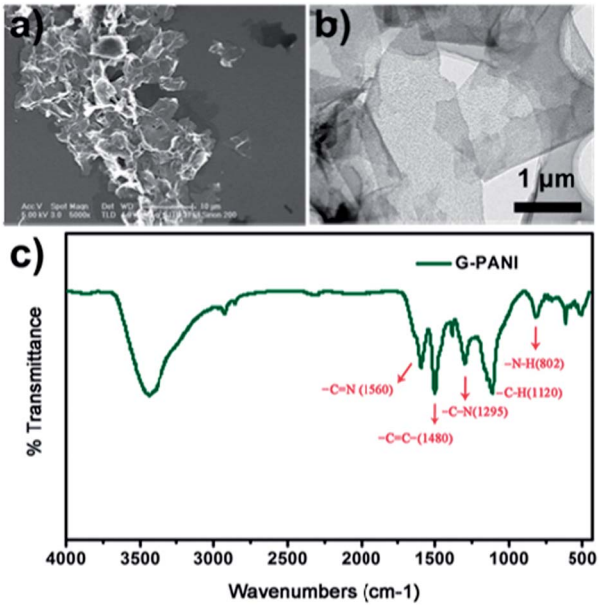

Fig. 1 (a) SEM, (b) TEM micrographs, and (c) FT-IR spectrum of the G–PANI nanosheets.

The mixtures were cooled down from an isotropic phase to a chiral nematic phase at a cooling rate of 0.5 K min^{-1} to observe the phase transition temperature. The cells were cured at the blue phase under ultraviolet light with an intensity of 3 mW cm^{-2} for 10 minutes. Fig. 2(a) shows the platelet textures of the mixture under a polarized optical microscope (POM, XPL-30TF) and its phase transition process. Fig. 2(b) is an experimental setup to measure the electro-optic properties of the polymer-stabilized BPLC. In order to obtain a collimated light, the light source was focused into an optic fiber. The IPS cell applied with a 1 kHz square-wave AC signal was placed between two crossed polarizers. The transmittance was measured using a detector connected with a spectrometer.

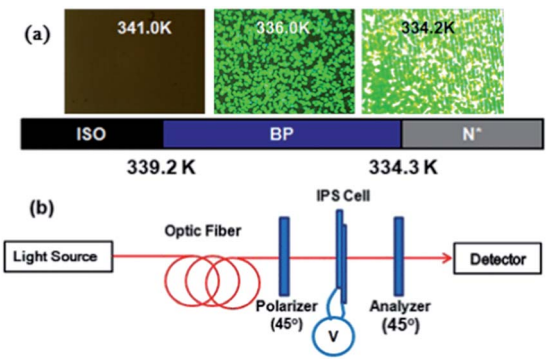

Fig. 2 (a) Phase transition of blue phase liquid crystals without G–PANI from the isotropic phase (ISO) to the chiral nematic phase (N*) and texture under POM and (b) experimental setup for electro-optic measurement of the IPS cell.

Results and discussion

Mesomorphic behavior

To compare the effects of G–PANI and graphene, another group of samples with different concentrations of graphene was prepared. The mesomorphic behaviors of different concentrations of G–PANI and graphene doped into BPLCs were studied by using a polarized optical microscope and a temperature controller. Fig. 3 shows the platelet textures of different concentrations of G–PANI and graphene doped into BPLC samples at 337 K, respectively. It was observed that the platelet textures of BPLCs doped with different concentrations of G–PANI and graphene were similar. Fig. 4 shows the platelet textures of BPLC samples with 0.05 wt% of G–PANI and graphene after polymer stabilization at different temperatures, respectively. The platelet texture was observed in a temperature range of 253–339.3 K after polymer stabilization.

For comparison, precursors with different concentrations of G–PANI and graphene were prepared as listed in Tables 1 and 2, respectively. It was observed that the blue phase temperature ranges of mixtures doped with different concentrations of G–PANI and graphene have almost no change.

Driving characteristics

Fig. 5 depicts the measured voltage-dependent (V–T) curve of the mixtures with different concentrations of G–PANI and graphene after polymer stabilization at room temperature, respectively. The transmittance of 100% was calibrated by that of the cell under crossed polarizers at the on-state voltage and

Table 1 The temperature range of BPLC samples before and after the polymer stabilization with different concentrations of G–PANI

Sample	G–PANI, wt%	ΔT/K (before UV)	ΔT/K (after UV)
1	0	4.9	>85
2	0.03	4.8	>85
3	0.05	5.0	>85
4	0.10	5.6	>85
5	0.20	5.2	>85
6	0.50	4.7	>85
7	1.00	5.7	>85
8	1.50	6.6	>85
9	2.00	6.5	>85

Table 2 The transition temperatures of BPLC samples with different concentrations of graphene

Sample no.	Graphene, wt%	ΔT/K (before UV)	ΔT/K (after UV)
A	0	5.2	>85
B	0.05	5.1	>85
C	0.10	5.2	>85
D	0.20	5.3	>85

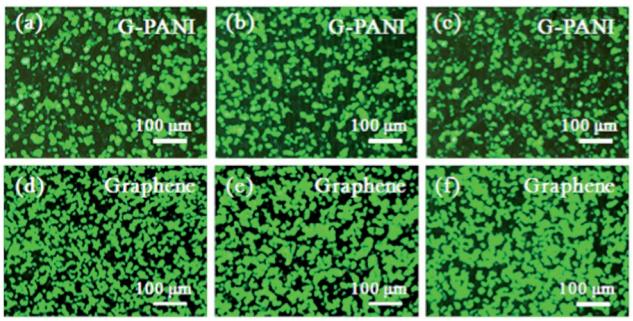

Fig. 3 POM images of (a) 0.00 wt%, (b) 0.05 wt%, and (c) 1.00 wt% of G–PANI and (d) 0.00 wt%, (e) 0.05 wt%, and (f) 1.00 wt% of graphene dispersed BPLCs at 337 K, respectively.

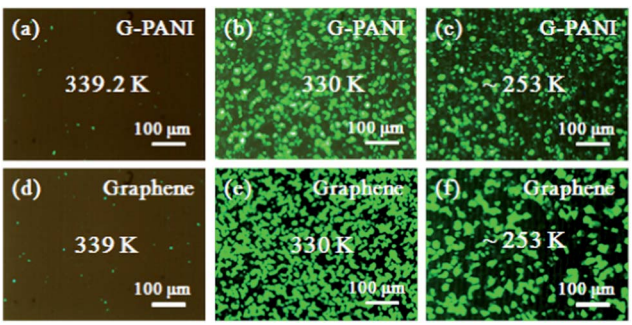

Fig. 4 Platelet textures of BPLC samples with 0.05 wt% of G–PANI and graphene after polymer stabilization at different temperatures.

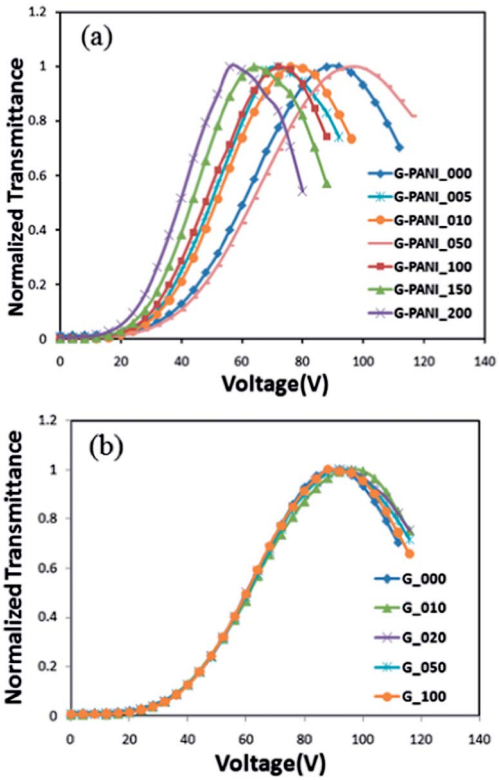

Fig. 5 Voltage–transmittance curve of the PS-BPLC doped with different concentrations of (a) G–PANI and (b) graphene at room temperature after polymer stabilization.

the transmittance of 0% was calibrated by that of the cell under crossed polarizers at the off-state voltage. Fig. 6 shows the Kerr constant fitted by the extended Kerr effect.[33] With the concentration of the G–PANI dopant increasing from 0 wt% to 0.05 wt%, the Kerr constant of the composites increases. As the G–PANI nanosheets can be wrapped by the polymer network around the disclination lines of blue phase liquid crystals, the conductivity of the material system will increase resulting in the improvement of the Kerr constant. However, the Kerr constant of samples decreases when the concentration of the G–PANI dopant increased from 0.05 wt% to 0.50 wt%. With the increase of concentration of G–PANI, the effect of conductivity increase is offset by the growth in the quantity of the polymer mixture. Therefore, the driving performance of the material is degraded. Finally, when the concentration of G–PANI is higher than 0.50 wt%, the Kerr constant increases with the concentration of the G–PANI dopant. Because the G–PANI wrapped by polymer is saturated if the concentration of G–PANI is too high, the rest of G–PANI is dispersed into the mixture uniformly, which leads to the large increase of the mixture conductivity. Therefore, the Kerr constant increases with the concentration of G–PANI.

According to the explanation above, when the concentration of G–PANI is less than 0.05 wt% or higher than 0.50 wt%, the Kerr constant increases with the concentration of G–PANI. As the concentration of G–PANI increases, the conductivity of PS-BPLC system will increase. However, if the conductivity of PS-BPLC system is relatively high, the voltage holding ratio (VHR) in each pixel will degrade significantly[34] in spite of the fact that the driving capability can be greatly improved. Therefore, the optimal G–PANI concentration should be less than 0.2 wt%, considering the effect to Kerr constant and VHR of PS-BPLC comprehensively.

For comparison, the BPLCs mixtures doped with different concentrations of graphene were also prepared. As shown in Fig. 5(b) and 6, the *V–T* curve and Kerr constant of the samples doped with different concentrations of graphene have almost no change compared to the samples without the graphene dopant. Therefore, the change of the electro-optical properties of the samples doped with different concentrations of G–PANI comes from the increase of the conductivity introduced by PANI, but not graphene, which is just in order to tackle the aggregation of polyaniline while retaining the overall high conductivity and good dispersity.

Fig. 7 depicts the hysteresis and residual birefringence as a function of the concentration of G–PANI. Hysteresis is defined as the difference in voltage at the half-maximum transmittance between the forward and backward directions which is divided by the saturation voltage.[35] Residual birefringence is defined as the remaining transmittance of the backward operation at 0 V.[36] It is clear that when the concentration of G–PANI is less than 0.50 wt%, both hysteresis and residual birefringence do not change. However, if the concentration of G–PANI is higher than 0.50 wt%, both hysteresis and residual birefringence of PS-BPLCs increase with increasing concentration of G–PANI. Similar to the analysis of the driving issue, when the concentration of G–PANI is higher than 0.50 wt%, the G–PANI wrapped by polymer is saturated and the rest of G–PANI is dispersed into the mixture uniformly resulting in the increase of the mixture conductivity. Therefore, with the same applied electric field, the lattice distortion is more severe compared to the mixture with low concentrations of the G–PANI dopant. After the applied electric field is removed, the LC molecules around the G–PANI dispersed into the mixture cannot recover to their original state due to the distorted lattice, resulting in the increase of residual birefringence. Therefore, both hysteresis and birefringence increase with the concentration of G–PANI.

Response time

For PS-BPLCs, the fast response time is an attractive feature. As the rise time is related to the driving voltage, we only evaluate the decay time which was performed from the on-state voltage to 0 V. The decay times of the samples with different concentrations of G–PANI were measured at room temperature. As shown in Fig. 8, when the concentration of G–PANI is less than 0.50 wt%, the decay time of samples almost have no change because the rotational viscosity and elastic constant of the material are not affected with such a low concentration of G–PANI. However, if the concentration of G–PANI is higher than 0.50 wt%, the G–PANI wrapped by the polymer is saturated and the rest of G–PANI is dispersed into the mixture uniformly,

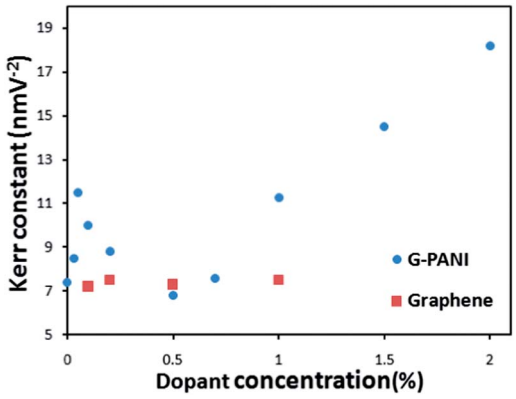

Fig. 6 Kerr constant of PS-BPLC with different concentrations of G–PANI and graphene.

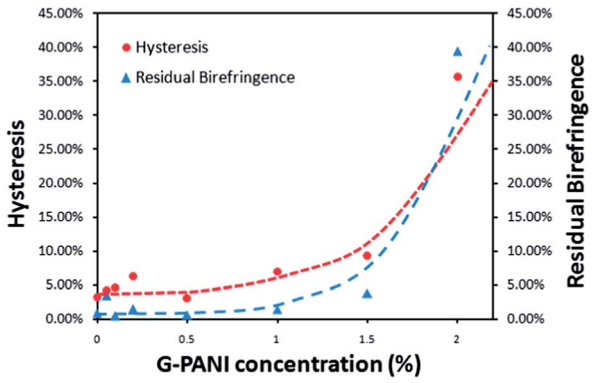

Fig. 7 Hysteresis and residual birefringence of BPLCs doped with different concentrations of G–PANI.

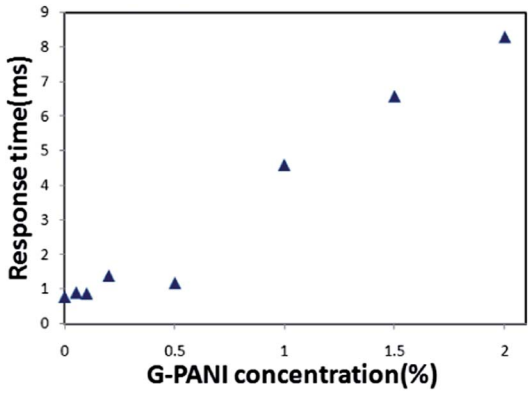

Fig. 8 Decay time of the samples with different concentrations of G–PANI.

which leads to the increase of rotational viscosity of the mixtures. Therefore, the decay time of the samples increases gradually with the concentration of G–PANI.

Conclusions

In summary, a small amount of polyaniline functionalized graphene nanosheets (G–PANI, 0.03–2.00 wt%) doped into the polymer-stabilized blue phase liquid crystal (PS-BPLC) shows significant effects on the driving voltage of the mixtures. G–PANI nanosheets can be wrapped by the polymer network around the disclination lines of the blue phase liquid crystal, so the effective electric field of BPLC materials will increase. At relatively low concentrations (less than 0.05 wt%) of G–PANI, the Kerr constant of the mixtures increase by ~55% in comparison with that of PS-BPLC without G–PANI. Meanwhile, the response time, the hysteresis and the residual birefringence are little affected. However, at relatively high G–PANI contents (more than 0.50 wt%), the response time, the hysteresis and the residual birefringence degrade significantly in spite of the fact that the driving capability can be greatly improved.

Acknowledgements

This work was supported in part by 973 Program (2013CB328804) and NSFC (61275026).

Notes and references

1 S. Meiboom, J. P. Sethna, P. W. Anderson and W. F. Brinkman, *Phys. Rev. Lett.*, 1981, **46**, 1216.
2 R. Memmer, *Liq. Cryst.*, 2000, **27**, 533.
3 H. Kikuchi, M. Yokota, Y. Hisakado, H. Yang and T. Kajiyama, *Nat. Mater.*, 2002, **1**, 64.
4 K. M. Chen, S. Gauza, H. Xianyu and S. T. Wu, *J. Disp. Technol.*, 2010, **6**, 49.
5 M. Kim, B. G. Kang, M. S. Kim, M. K. Kim, P. Kumar, M. H. Lee, S. W. Kang and S. H. Lee, *Curr. Appl. Phys.*, 2010, **10**, 118.
6 J. Yan, Y. Li and S. T. Wu, *Opt. Lett.*, 2011, **36**, 1404.
7 S. Y. Lu and L. C. Chien, *Opt. Lett.*, 2010, **35**, 562.
8 J. L. Zhu, J. G. Lu, J. Qiang, E. W. Zhong, Z. C. Ye, Z. H. He, X. J. Guo, C. Y. Dong, Y. K. Su and H. P. D. Shieh, *J. Appl. Phys.*, 2012, **111**, 033101.
9 H. Q. Cui, Z. C. Ye, W. Hu, X. W. Lin, T. C. Chung, T. S. Jen and Y. Q. Lu, *J. Inf. Disp.*, 2011, **12**, 115.
10 H. Coles and S. Morris, *Nat. Photonics*, 2010, **4**, 676.
11 S. Yokoyama, S. Mashiko, H. Kikuchi, K. Uchida and T. Nagamura, *Adv. Mater.*, 2006, **18**, 48.
12 H. Iwamochi and A. Yoshizawa, *Appl. Phys. Express*, 2008, **1**, 111801.
13 K. M. Chen, S. Gauza, H. Xianyu and S. T. Wu, *J. Disp. Technol.*, 2010, **6**, 318.
14 L. Wang, W. He, X. Xiao, M. Wang, M. Wang, P. Yang, Z. Zhou, H. Yang, H. Yu and Y. Lu, *J. Mater. Chem.*, 2012, **22**, 19629.
15 L. Wang, W. He, X. Xiao, F. Meng, Y. Zhang, P. Yang, L. Wang, J. Xiao, H. Yang and Y. Lu, *Small*, 2012, **8**, 2189.
16 L. Rao, J. Yan, S. T. Wu, S. Yamamoto and Y. Haseba, *Appl. Phys. Lett.*, 2011, **98**, 081109.
17 Y. Chen, D. Xu, S. T. Wu, S. Yamamoto and Y. Haseba, *Appl. Phys. Lett.*, 2013, **102**, 141116.
18 J. L. Zhu, S. B. Ni, Y. Song, E. W. Zhong, Y. J. Wang, C. P. Chen, Z. C. Ye, G. F. He, D. Q. Wu, X. L. Song, J. G. Lu and Y. K. Su, *Appl. Phys. Lett.*, 2013, **102**, 071104.
19 L. Rao, J. Yan, S. T. Wu and S. H. Lee, *Appl. Phys. Lett.*, 2009, **95**, 231101.
20 M. Kim, M. S. Kim, B. G. Kang, M. K. Kim, S. Yoon, S. H. Lee, Z. Ge, L. Rao, S. Gauza and S. T. Wu, *J. Phys. D: Appl. Phys.*, 2009, **42**, 235502.
21 M. Jiao, Y. Li and S. T. Wu, *Appl. Phys. Lett.*, 2010, **96**, 011102.
22 H. C. Cheng, J. Yan, T. Ishinabe and S. T. Wu, *Appl. Phys. Lett.*, 2011, **98**, 261102.
23 S. Yang, X. Feng, L. Wang, K. Tang, J. Maier and K. Müllen, *Angew. Chem., Int. Ed.*, 2010, **49**, 4795.
24 A. Fasolino, J. H. Los and M. I. Katsnelson, *Nat. Mater.*, 2007, **6**, 858.
25 A. A. Balandin, S. Ghosh, W. Bao, I. Calizo, D. Teweldebrhan, F. Miao and C. N. Lau, *Nano Lett.*, 2008, **8**, 902.
26 A. K. Geim and K. S. Novoselov, *Nat. Mater.*, 2007, **6**, 183.
27 M. J. Allen, V. C. Tung and R. B. Kaner, *Chem. Rev.*, 2010, **110**, 132.
28 Y. Hernandez, V. Nicolosi, M. Lotya, F. M. Blighe, Z. Sun, S. De, I. T. McGovern, B. Holland, M. Byrne, Y. K. Gun'Ko, J. J. Boland, P. Niraj, G. Duesberg, S. Krishnamurthy, R. Goodhue, J. Hutchison, V. Scardaci, A. C. Ferrari and J. N. Coleman, *Nat. Nanotechnol.*, 2008, **3**, 563.
29 Z. Wang, J. Liu, W. Wang, H. Chen, Z. Liu, Q. Yu, H. Zeng and L. Sun, *Chem. Commun.*, 2013, **49**, 10835.
30 Y. G. Wang, H. Q. Li and Y. Y. Xia, *Adv. Mater.*, 2006, **18**, 2619.
31 J.-L. Zhu, S.-B. Ni, E.-W. Zhong, J.-G. Lu and Y. Su, *Sym. Dig. Tech. (SID)*, 2012, **43**, 106.

32 S. Gilje, S. Han, M. Wang, K. L. Wang and R. B. Kaner, *Nano Lett.*, 2007, **7**, 3394.
33 J. Yan, H. C. Cheng, S. Gauza, Y. Li, M. Jiao, L. Rao and S. T. Wu, *Appl. Phys. Lett.*, 2010, **96**, 071105.
34 C. D. Tu, C. L. Lin, J. Yan, Y. Chen, P. C. Lai and S. T. Wu, *J. Disp. Technol.*, 2013, **9**, 3.
35 J. Yan and S. T. Wu, *J. Disp. Technol.*, 2011, **7**, 490.
36 C. Y. Fan, C. T. Wang and T. H. Lin, *Sym. Dig. Tech. (SID)*, 2011, **42**, 213.